Indication of Superconductivity at 35 K in Graphite-Sulfur Composites

R. Ricardo da Silva,* J. H. S. Torres, and Y. Kopelevich

Instituto de Física "Gleb Wataghin," Universidade Estadual de Campinas, Unicamp 13083-970, Campinas, São Paulo, Brasil
(Received 17 May 2001; published 12 September 2001)

We report magnetization measurements performed on graphite-sulfur composites which demonstrate a clear superconducting behavior below the critical temperature $T_{c0} = 35$ K. The Meissner-Ochsenfeld effect, screening supercurrents, and magnetization hysteresis loops characteristic of type-II superconductors were measured. The results indicate that the superconductivity occurs in a small sample fraction, possibly related to the sample surface.

A considerable scientific interest of graphite and graphite-based superconducting compounds [1–5] has been renewed [6–8] by the discovery of superconductivity at 39 K in MgB_2 [9], a material similar to graphite both electronically and crystallographically. Besides, recent experiments [10–12] suggested the occurrence of superconducting correlations in highly oriented pyrolitic graphite samples. It has been proposed [13] that a topological disorder in graphene sheets can trigger the superconducting instabilities.

In the present paper, we report an unambiguous evidence for the superconductivity occurrence in graphite-sulfur (C-S) composite samples. A clear superconducting behavior is found below the critical temperature $T_{c0} = 35$ K.

The C-S composites were prepared by mixture of the graphite powder consisting of ∼8 μm size particles [the impurity content in ppm: Fe (32), Mo (<1), Cr (1.1), Cu (1.5)] and the sulfur powder (99.998%; Aldrich Chemical Company, Inc.) in a mass ratio m_C:m_S = 1:1 (m_C = 0.5 g, m_S = 0.5 g), where m_C and m_S are the graphite and the sulfur masses, respectively. The mixture was pressed into pellets, held under Ar atmosphere at 650 K for 1 h and, subsequently, annealed at 400 K for 10 h before cooling to room temperature. During the heat treatment, 0.35 g of the sulfur was evaporated, i.e., the final sulfur contents in the composite was 23 wt%.

dc magnetization and low-frequency ($\nu = 1$ Hz) standard four-probe resistance measurements were performed on the sample of size $4.86 \times 4.52 \times 3.52$ mm^3 by means of SQUID magnetometer MPMS5 and PPMS commercial equipment (Quantum Design).

X-ray (θ-2θ geometry) analysis revealed a small decrease in the c-axis lattice parameter of the hexagonal graphite from c = 6.721 Å in the pristine graphite powder to c = 6.709 Å in the composite sample, and no changes in the lattice parameters of the orthorhombic sulfur (a = 10.45 Å, b = 12.84 Å, c = 24.46 Å). Figure 1 shows the x-ray diffraction pattern of C—23 wt% S composite obtained with Cu Kα source and 2θ step of 0.05°. As Fig. 1 illustrates, no impurity or additional phases were found.

Figure 2 presents temperature dependencies of the magnetization $M(T, H) = m(T, H)/V$ (m is the sample magnetic moment and V is the sample volume) measured in the as-received sample (labeled here as A) at applied fields $H = 10$ and 100 Oe. The magnetization data corresponding to the zero-field-cooled (ZFC) regime, $M_{ZFC}(T)$, were taken on heating after the sample cooling at zero applied field, and the magnetization in the field-cooled on cooling (FCC) regime, $M_{FCC}(T)$, was measured as a function of decreasing temperature in the applied field. Figure 2 demonstrates a pronounced difference between $M_{ZFC}(T)$ and $M_{FCC}(T)$ which occurs with the temperature decreasing. The inset of Fig. 2 gives a detailed view of the data obtained for $H = 100$ Oe in a vicinity of the $T_c(H = 100$ Oe$) = 33$ K below which a departure of $M_{ZFC}(T)$ from $M_{FCC}(T)$ takes place. As can be seen from this plot, both $M_{ZFC}(T)$ and $M_{FCC}(T)$ become more diamagnetic at $T < T_c(H)$. Such magnetization behavior is characteristic of superconductors: The enhancement of the diamagnetism below the superconducting transition temperature $T_c(H)$ originates from the screening supercurrents (ZFC regime) and the Meissner-Ochsenfeld effect of magnetic flux expulsion (FCC regime). It can also be seen in Fig. 2 that, as the applied field increases, the normal state orbital diamagnetism of graphite overcomes a positive contribution to the magnetization (which can be due to both intrinsic weak ferromagnetism of graphite [11,13,14] and magnetic impurities) resulting in a negative total magnetization above T_c.

Figure 3 depicts the normalized ZFC magnetization $M(T)/|M(50$ K$)|$ measured for various applied fields demonstrating that the transition temperature $T_c(H)$ decreases with the field increasing as well as that $H = 10$ kOe completely suppresses the superconducting response. The obtained $T_c(H)$ is given in the magnetic field-temperature (H-T) plane (Fig. 4).

Figure 5(a) presents the magnetization hysteresis loop $M(H)$ measured at $T = 6$ K after cooling the sample from 300 K to the target temperature in a zero applied field. In Fig. 5(b) we show the same data after subtraction of a diamagnetic background signal. Figures 5(a) and 5(b)
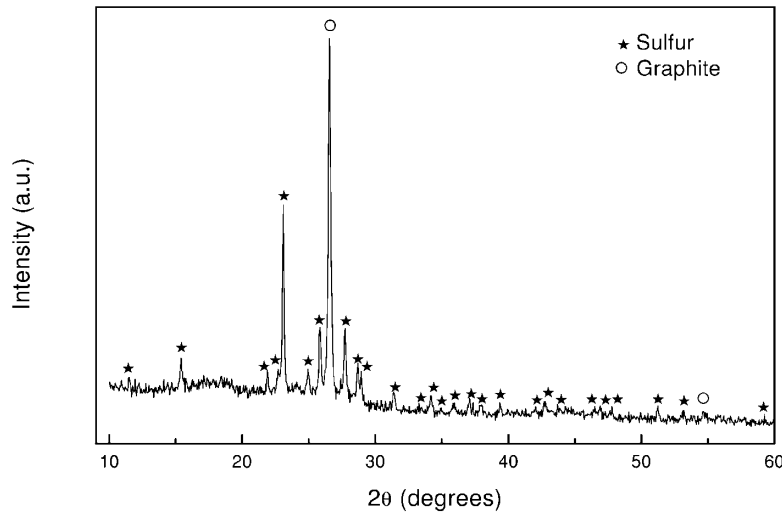
FIG. 1.   X-ray θ-2θ diffraction pattern of the C—23 wt% S composite.

provide unambiguous evidence that our sample is a type-II superconductor with a strong vortex pinning [15,16].

In contrast to alkali-metal-doped graphite samples in which the superconductivity vanishes after a short-time sample annealing at $T \geq 100$ K [3], the superconducting properties in our sample were stable during one week of measurements in the temperature range 5 K $\leq T \leq$ 300 K. To verify further the superconductivity stability, the sample was kept at ambient conditions for two weeks. During this time, the sample has lost about 4 wt% of sulfur. Then, we found a small decrease in $T_c(H)$ and a strong reduction in magnitude of the superconducting response. Figure 6(a) exemplifies $M_{ZFC}(T)$ and $M_{FCC}(T)$ recorded for this sample (labeled here as B) in applied field $H = 100$ Oe, and Fig. 6(b) presents a $M(H)$ hys-

teresis loop obtained at $T = 6$ K. The transition temperature $T_c(H)$ measured in sample B for several H is shown in Fig. 4.

It is tempting to relate $H(T_c)$, shown in Fig. 4, to the upper critical field boundary. However, a different interpretation is also possible. It is found that $H(T_c)$ obtained for sample A can be best described by the power law,

$$H = H^*(1 - T_c/T_{c0})^{3/2}, \qquad (1)$$

in a vicinity of $T_{c0} = 35$ K, and by the equation,

$$H = H_0 \exp(-T_c/T_0), \qquad (2)$$

below a reduced temperature $T/T_{c0} \sim 0.8$, where $H_0 = 5$ T and $T_0 = 7$ K (see Fig. 4). Equations (1) and (2)
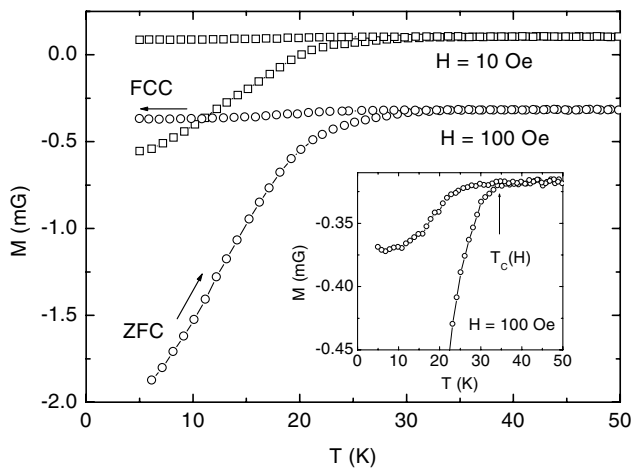

FIG. 2.   Temperature dependencies of the magnetization $M(T)$ measured in as-received sample A in zero-field-cooled (ZFC) and field-cooled on cooling (FCC) regimes at two applied fields; 10 and 100 Oe. Inset gives enlarged view of the superconducting transition recorded at $H = 100$ Oe.
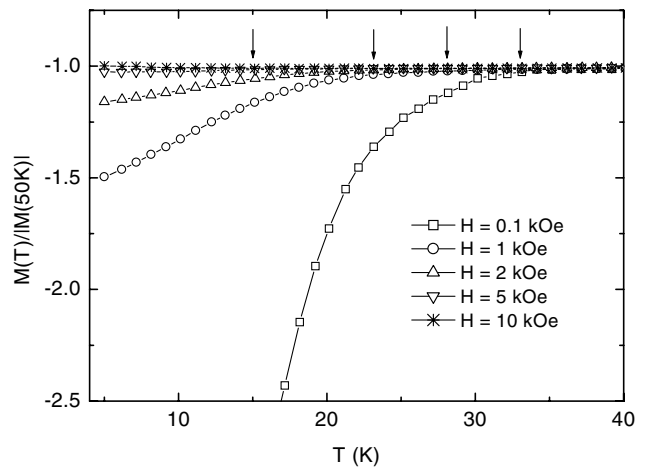

FIG. 3.   Normalized ZFC magnetization measured in sample A at various applied fields. Arrows denote the superconducting transition temperature $T_c(H)$ below which a departure of $M_{ZFC}(T)$ from $M_{FCC}(T)$ takes place, as shown in the inset of Fig. 2.
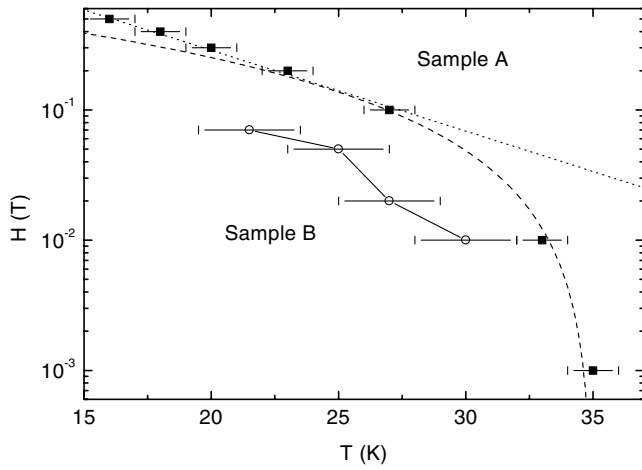
FIG. 4. $H(T_c)$ for samples A and B. Dashed line and dotted line are obtained from Eqs. (1) and (2) with the fitting parameters $T_{c0} = 35$ K, $H^* = 0.9$ T, $T_0 = 7$ K, and $H_0 = 5$ T.

imply that $T_c(H)$ can be accounted for by the existence of a breakdown field $H_b(T)$ which destroys the superconductivity induced by a proximity effect [17–19]. According to the theory [19], $H_b(T)$ for normal-metal-superconductor structures saturates in the limit $T \rightarrow 0$ to the value $H_b(T = 0) \approx 0.37 H_0$. Taking $H_0 = 5$ T, one gets $H_b(T = 0) = 1.85$ T which agrees with the

experimentally determined field $H = 1$ T at which the superconducting response vanishes (see Fig. 3).

The zero-field resistivity $\rho(T)$ measurements performed on sample A (see Fig. 7) revealed a slight increase ($\sim$20%) of the resistivity lowering temperature from 300 K to $T_{on} \approx T_{c0} = 35$ K, and its logarithmic divergence [$\rho(T) \sim \ln(T_{0B}/T)$] with a further temperature decrease, $T \leq T_{on}$. The obtained $\rho(T)$ at $T \leq T_{c0}$ resembles the resistivity behavior in two-dimensional superconductors in the regime of weakly localized Cooper pairs [20]. While we cannot rule out completely other (fermionic) mechanisms, the coincidence of T_{on} and T_{c0} as well as the obtained low value of $T_{0B} = 5$ K support the bosonic resistivity behavior [20] at $T \leq T_{c0}$.

Taking the magnetization and resistivity data together, one arrives at the conclusion that the superconductivity in our samples is localized within "grains" or "islands" large enough to carry vortices. Note that the magnetic hysteresis associated with the flux trapping can occur in materials which consist of the superconducting elements each smaller than the penetration depth [21].

The magnetization data presented in Fig. 2 demonstrate that the superconducting shielding effect is associated with a small volume fraction of the sample ($\sim$0.05% of that
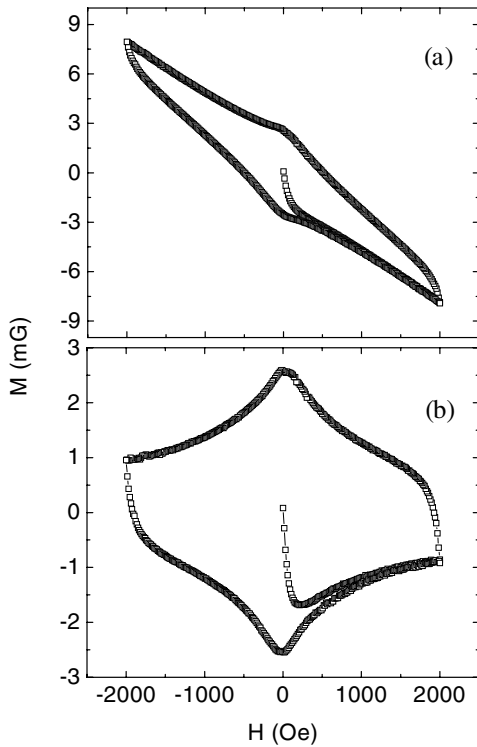

FIG. 5.   (a) Magnetization hystereis loop $M(H)$ measured in sample A at $T = 6$ K; (b) $M(H)$ obtained after subtraction of the diamagnetic background signal $M = -\chi H$ with $\chi = 3.5 \times 10^{-3}$ mG/Oe.
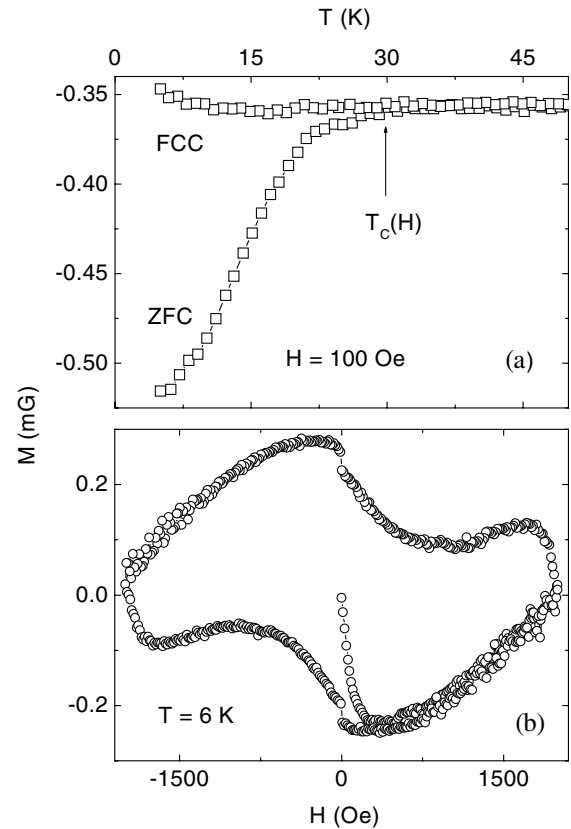

FIG. 6.   (a) $M(T)$ measured in sample B in ZFC and FCC regimes at $H = 100$ Oe; (b) Magnetization hysteresis loop obtained for sample B at $T = 6$ K after subtraction of the diamagnetic background signal $M = -\chi H$ with $\chi = 3.5 \times 10^{-3}$ mG/Oe (6 K).
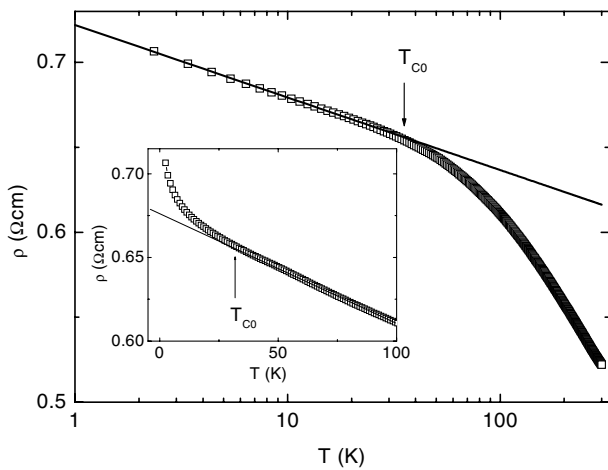
FIG. 7. Semilogarithmic plot of zero-field resistivity $\rho(T)$ measured in sample A; solid line is obtained from the equation $\rho(T) = 0.6922 + 0.01855 \times \ln(T_{0B}/T)$, where $T_{0B} = 5$ K. Inset shows linear plot of the same data in a vicinity of $T_{c0} = 35$ K; solid line is only a guide.

expected for a bulk ideal superconductor) which is compatible with the small size of the "islands."

We note further that $T_c(H)$ measured in samples A and B differs by a few kelvin only (see Fig. 4), whereas the superconducting shielding effect as well as the magnetization hysteresis width are strongly suppressed in sample B. These results can be understood assuming that the size of superconducting islands in sample B is much smaller than that in sample A.

Finally, we stress that no sign of the superconductivity was found in our pristine graphite powder. On the other hand, the highest $T_c = 17$ K in sulfur was reached under a pressure of 160 GPa [22]. We speculate that the superconductivity in C-S composites originates from a sulfur-carbon interaction at the graphite surface. Similar to the effect of adsorbed gases [23,24], a hybridization between carbon and sulfur can increase the local charge density and therefore trigger the superconductivity. Further studies should verify this hypothesis.

In conclusion, the above results provide an unambiguous evidence for the occurrence of high-temperature superconductivity in graphite-sulfur composite samples and open new perspectives for the engineering of graphite-based superconductors with high T_c. Recently, C-S composites with T_c exceeding 35 K have been obtained [25].

*Also at FAENQUIL, 126000-000, Lorena, SP, Brasil.

[1] N. B. Hannay, T. H. Geballe, B. T. Matthias, K. Andres, P. Schmidt, and D. MacNair, Phys. Rev. Lett. **14**, 225 (1965).

[2] Y. Koike, S.-I. Tanuma, H. Suematsu, and K. Higuchi, J. Phys. Chem. Solids **41**, 1111 (1980).

[3] I. T. Belash, A. D. Bronnikov, O. V. Zharikov, and A. V. Palnichenko, Solid State Commun. **64**, 1445 (1987); **69**, 921 (1989).

[4] A. Chaiken, M. S. Dresselhaus, T. P. Orlando, G. Dresselhaus, P. M. Tedrow, D. A. Neumann, and W. A. Kamitakahara, Phys. Rev. B **41**, 71 (1990).

[5] R. A. Jishi and M. S. Dresselhaus, Phys. Rev. B **45**, 12 465 (1992).

[6] K. D. Belashchenko, M. van Schilfgaarde, and A. P. Antropov, cond-mat/0102290.

[7] J. M. An and W. E. Pickett, Phys. Rev. Lett. **86**, 4370 (2001).

[8] G. Baskaran, cond-mat/0103308.

[9] J. Nagamatsu, N. Nakagawa, T. Muranaka, Y. Zenitani, and J. Akimitsu, Nature (London) **410**, 63 (2001).

[10] Y. Kopelevich, V. V. Lemanov, S. Moehlecke, and J. H. S. Torres, Fiz. Tverd. Tela (St. Petersburg) **41**, 2135 (1999) [Sov. Phys. Solid State **41**, 1959 (1999)].

[11] Y. Kopelevich, P. Esquinazi, J. H. S. Torres, and S. Moehlecke, J. Low Temp. Phys. **119**, 691 (2000).

[12] H. Kempa, Y. Kopelevich, F. Mrowka, A. Setzer, J. H. S. Torres, R. Höhne, and P. Esquinazi, Solid State Commun. **115**, 539 (2000).

[13] J. González, F. Guinea, and M. A. H. Vozmediano, Phys. Rev. B **63**, 134421 (2001).

[14] D. V. Khveshchenko, cond-mat/0101306.

[15] Y. B. Kim, C. F. Hempstead, and A. R. Strnad, Phys. Rev. **129**, 528 (1963).

[16] Y. Yeshurun, A. P. Malozemoff, and A. Shaulov, Rev. Mod. Phys. **68**, 911 (1996).

[17] G. Deutscher and P. G. de Gennes, in *Superconductivity,* edited by R. Parks (Dekker, New York, 1969), Vol. 2.

[18] G. Deutscher and A. Kapitulnik, Physica (Amsterdam) **168A**, 338 (1990).

[19] A. L. Fauchère and G. Blatter, Phys. Rev. B **56**, 14 102 (1997).

[20] D. Das and S. Doniach, Phys. Rev. B **57**, 14 440 (1998).

[21] C. Ebner and D. Stroud, Phys. Rev. B **31**, 165 (1985), and references therein.

[22] V. V. Struzhkin, R. J. Hemley, H.-K. Mao, and Y. A. Timofeev, Nature (London) **390**, 382 (1997).

[23] S. M. Lee, Y. H. Lee, Y. G. Hwang, J. R. Hahn, and H. Kang, Phys. Rev. Lett. **82**, 217 (1999).

[24] P. Ruffieux, O. Gröning, P. Schwaller, L. Schlapbach, and P. Gröning, Phys. Rev. Lett. **84**, 4910 (2000).

[25] S. Moehlecke, Pei-Chun Ho, and M. B. Maple (to be published).